



TITLE:

Magnetic fluctuations and superconductivity
in $\text{LaFeAsO}_{1-x}\text{F}_x$ under pressure as
seen via ^{75}As NMR

AUTHOR(S):

Nakano, T.; Fujiwara, N.; Kamihara, Y.; Hirano, M.;
Hosono, H.; Okada, H.; Takahashi, H.

CITATION:

Nakano, T. ...[et al]. Magnetic fluctuations and superconductivity in $\text{LaFeAsO}_{1-x}\text{F}_x$ under pressure as seen via ^{75}As NMR. Physical Review B 2010, 82(17): 172502.

ISSUE DATE:

2010-11

URL:

<http://hdl.handle.net/2433/134551>

RIGHT:

© 2010 The American Physical Society

Magnetic fluctuations and superconductivity in $\text{LaFeAsO}_{1-x}\text{F}_x$ under pressure as seen via ^{75}As NMR

T. Nakano,¹ N. Fujiwara,^{1,*} Y. Kamihara,^{2,3,†} M. Hirano,⁴ H. Hosono,^{3,4} H. Okada,^{2,5,‡} and H. Takahashi^{2,5}

¹Graduate School of Human and Environmental Studies, Kyoto University, Yoshida-Nihonmatsu-cho, Sakyo-ku, Kyoto 606-8501, Japan

²TRI-P, Japan Science and Technology Agency (JST), Sanban-cho bldg. 5, Sanban-cho, Chiyoda-ku, Tokyo 102-0075, Japan

³Materials and Structures Laboratory (MSL), Tokyo Institute of Technology, 4259 Nagatsuda, Midori-ku, Yokohama 226-8503, Japan

⁴Frontier Research Center (FRC), Tokyo Institute of Technology, 4259 Nagatsuda, Midori-ku, Yokohama 226-8503, Japan

⁵Department of Physics, College of Humanities and Sciences, Nihon University, Sakurajosui, Setagaya-ku, Tokyo 156-8550, Japan

(Received 29 September 2010; published 4 November 2010)

The relationship between antiferromagnetic (AF) fluctuation and superconductivity was investigated in the La1111 series, $\text{LaFeAsO}_{1-x}\text{F}_x$ ($x=0, 0.05, 0.08, 0.10$, and 0.14) by examining nuclear relaxation rates ($1/T_1$) at both ambient pressure and 3.0 GPa. The results show that the critical doping level at which low-frequency AF fluctuation vanishes is around the optimally doped regime ($x \sim 0.10$). Although the AF fluctuation is enhanced by applying pressure in the underdoped regime ($0.05 \leq x < 0.10$), the increase in critical transition temperature (T_c) is small, whereas T_c remarkably increases in the overdoped regime ($x=0.14$), implying that the AF fluctuation is less important to the high- T_c mechanism than the density of states at the electron pocket. The x dependence of T_c at 3.0 GPa is similar to that of R1111 ($\text{R}=\text{Ce}, \text{Pr}, \text{Nd}$, etc.) with $T_c \geq 40$ K at ambient pressure. The relationship between T_c and the pnictogen height or lattice constant indicates that pressure application is equivalent to full rare-earth substitution. This equivalence suggests that high T_c above 40 K is realized when the AF fluctuation is absent.

DOI: [10.1103/PhysRevB.82.172502](https://doi.org/10.1103/PhysRevB.82.172502)

PACS number(s): 74.70.Xa, 74.25.Ha, 74.62.Fj, 76.60.-k

Although a number of iron-based high- T_c superconductors are known, the 1111 series ($\text{RFeAsO}_{1-x}\text{F}_x$, $\text{R}=\text{Nd}, \text{Sm}, \text{Ce}$, and La , etc.) is highly important because its critical transition temperature (T_c) is relatively high compared to the 122 and 11 series.^{1–7} In the 1111 series, the optimal T_c is realized away from an antiferromagnetic (AF) phase on the T - x phase diagram, and the superconductivity is maintained even in a heavily doped regime. These features contrast with those of the 122 series, in which the optimal T_c appears adjacent to the AF phase.^{8–10} $\text{LaFeAsO}_{1-x}\text{F}_x$ is the initially discovered high- T_c pnictide and has inspired various investigations.¹ In the La1111 series, the optimal T_c of 26 K appears around $x=0.11$, away from the AF phase, and the superconducting (SC) phase survives even at $x=0.20$. The SC phase is sensitive to pressure, as in other iron-based pnictides, and shows a clear dome-shaped pressure dependence on the T - P phase diagram.^{11,12} The highest T_c is realized by applying pressure to optimally doped ($x \sim 0.11$) or heavily doped ($x \sim 0.14$) samples: T_c values, 26 and 20 K for $x=0.11$ and 0.14 , respectively, increase to 43 K at a pressure of 4–5 GPa.¹¹ Structurally, the highest T_c has been realized when Fe and As ions form regular tetrahedra or the pnictogen height above the basal plane of iron is high.^{13,14} Changes in these parameters resulting from pressure application can modify the band structure and covalency between Fe and As ions, affecting the electronic and/or magnetic properties. The origin of high T_c in iron-based pnictides is unclear; spin fluctuation seems to be an important factor from an analogy with high- T_c cuprates while an SC mechanism due to orbital fluctuation has also been suggested.^{15,16} To investigate whether the superconductivity is of magnetic origin as it is in high- T_c cuprates, we measured nuclear magnetic relaxation rates ($1/T_1$) of ^{75}As systematically under pressure for various doping levels ($x=0, 0.05, 0.08, 0.10$, and 0.14).

Powder samples were used for the nuclear magnetic reso-

nance (NMR) measurements of ^{75}As . Field-swept NMR spectra for the undoped and F-doped samples were measured at fixed frequencies of 35.1 and 45.1 MHz, respectively. The spectra exhibit a typical powder pattern with two peaks, which is seen under nuclear quadrupole interactions. The relaxation rate $1/T_1$ was measured at the lower field peak by the saturation-recovery method. The Fe-As planes contributing to this peak get aligned parallel to the applied field. Measurements at a pressure of 3.0 GPa were performed using a piston-cylinder-type pressure cell with FC-70 and 77 as a pressure-transmission liquid.

Figures 1(a)–1(d) show $1/T_1T$ measured at ambient pressure and 3.0 GPa for the samples doped with $x=0.05, 0.08, 0.10$, and 0.14 , where the AF phase is absent. The data in Figs. 1(b) and 1(d) were published in the previous work.²¹ Figure 2 shows $1/T_1T$ for undoped samples ($x=0$) together with those for the other doping levels. For the $x=0.14$ samples, $1/T_1T$ measured at 3.7 GPa is also plotted. At each doping level, qualitatively different features are revealed by applying pressure. Below, we describe in detail what occurs at each doping level using band calculations.^{17–19}

(1) *Lightly doped regime* ($x=0.05$). The T - x phase diagram at ambient pressure is shown in Fig. 3(a). Samples with a very low doping level exhibit clear Curie-Weiss behavior, suggesting that low-frequency AF fluctuation is predominant at this doping level. The Curie-Weiss behavior is enhanced and T_c increases slightly at a pressure of 3.0 GPa. The increase ΔT_c , indicated by arrows in Fig. 1(a), is estimated as 7–8 K. According to band calculations, the AF fluctuation originates from the nesting between hole and electron pockets, as illustrated in Fig. 1(e).

(2) *Underdoped regime* ($x=0.08$). For the $x=0.08$ samples, Curie-Weiss behavior is weaker than for $x=0.05$ and appears almost independent of T at ambient pressure. However, Curie-Weiss behavior returns when pres-

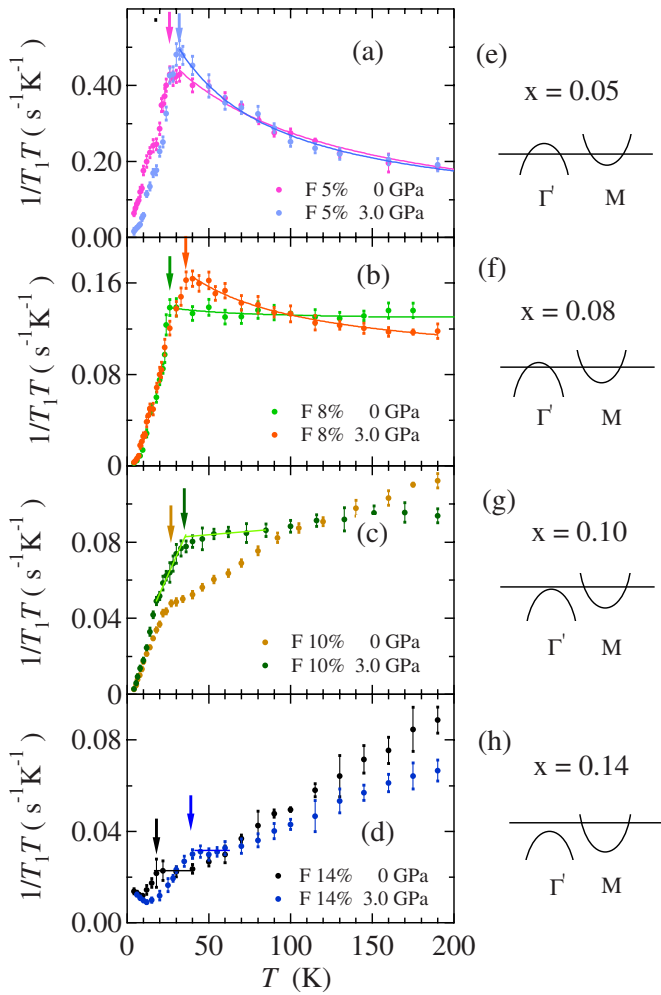


FIG. 1. (Color online) Relationship between AF fluctuation and band structure. [(a)–(d)] Temperature dependence of $1/T_1T$ at various doping levels. Arrows indicate T_c determined from changes in $1/T_1T$. [(e)–(h)] Schemes of electron and hole pockets. The Γ' point represents (π, π) in the unfolded Brillouin Zone. That point overlaps the Γ point corresponding to $(0, 0)$ in the original folded Brillouin Zone.

sure is applied. The increase in T_c is almost the same as for $x=0.05$. The weak Curie-Weiss behavior arises from weak nesting originating from an imbalance between hole and electron pockets [see Fig. 1(f)].

(3) *Optimally doped regime* ($x=0.10$). For the optimally doped samples ($x=0.10$), the Curie-Weiss behavior completely vanishes at both ambient pressure and 3.0 GPa. A drastic change due to pressure application is most clearly seen at this doping level. At ambient pressure, $1/T_1T$ shows a monotonous increase with increasing temperature. The behavior at temperatures above T_c originates not from the AF fluctuation but from peculiarities of the band structure.¹⁹ According to the band calculation, γ Fermi surface, a hole pocket near the $\Gamma'(\pi, \pi)$ point in the unfolded Brillouin zone, is sensitive to the doping level and vanishes around $x=0.10$, as illustrated in Fig. 1(g).^{14,19} Because the γ surface disappears, the AF fluctuation contributes slightly to $1/T_1T$. However, at high temperature states near the $\Gamma'(\pi, \pi)$ point just below the Fermi energy contribute to the density of

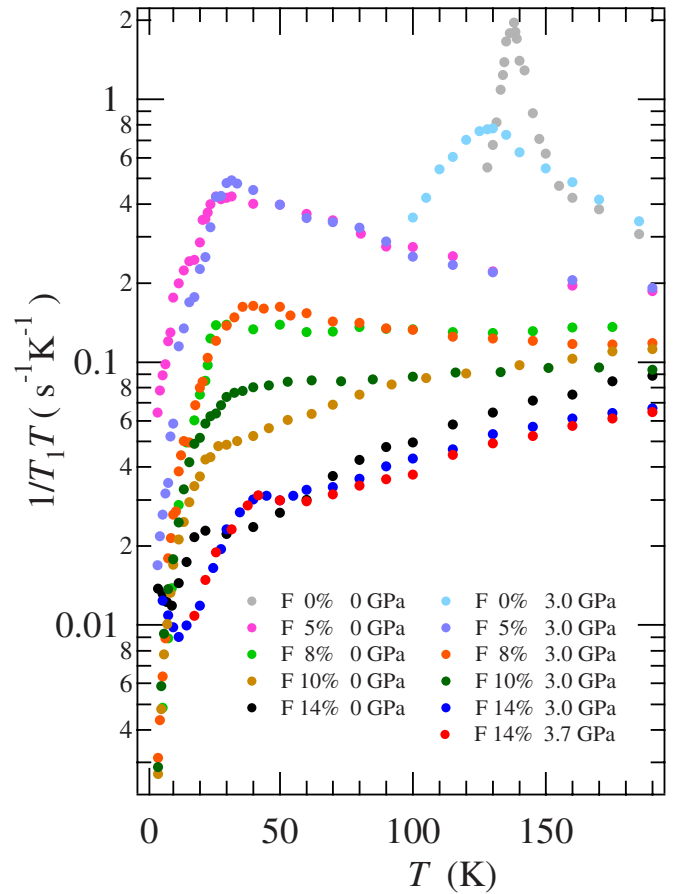


FIG. 2. (Color online) Temperature dependence of $1/T_1T$ for $x=0$ measured at ambient pressure and 3.0 GPa. Data shown in Figs. 1(a)–1(d) are also shown. For the $x=0.14$ samples $1/T_1T$ measured at 3.7 GPa is also plotted.

states $D(\varepsilon_F)$. The T -dependent $D(\varepsilon_F)$ gives rise to an increase in $1/T_1T$, which is expressed using the Korringa relation: $1/T_1T \propto D(\varepsilon_F)^2$. The spin part of the Knight shift is proportional to $D(\varepsilon_F)$. The T -dependent $D(\varepsilon_F)$ has been observed from measurements of the Knight shift.²⁰ At 3.0 GPa,

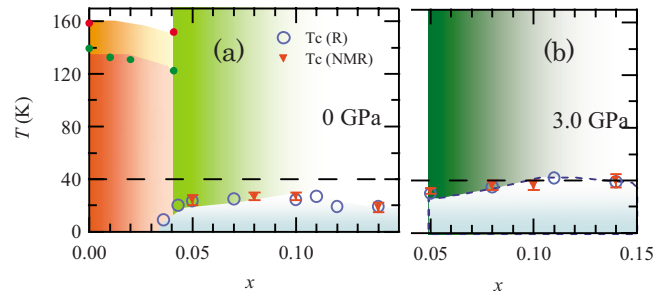


FIG. 3. (Color online) Phase diagram at ambient pressure and 3.0 GPa. Green area represents the region where low-frequency AF fluctuation is present: the darkness of the color indicates the strength of the AF fluctuation. Red closed triangles indicate T_c values determined from $1/T_1T$ in Figs. 1(a)–1(d) and blue open circles indicate those determined from the resistivity (Refs. 11 and 12). The tetragonal-to-orthorhombic phase transition temperatures, T_s , are indicated by red closed circles, and the AF transition temperatures, T_N , are indicated by green closed circles (Ref. 2).

$1/T_1T$ increases very slightly with the increase in temperature above T_c , and it resembles the case of $x=0.08$ at ambient pressure, implying that the weak T dependence at 3.0 GPa is attributable to the AF fluctuation. Applying a 3.0 GPa pressure changes the electronic state from a state free of AF fluctuation to one with AF fluctuation. The optimally doped regime ($x \sim 0.10$) is located on the boundary where the AF fluctuation vanishes.

(4) *Overdoped regime* ($x=0.14$). In the overdoped regime, the AF fluctuation is absent at both ambient pressure and 3.0 GPa. Instead, Korrington-type behavior, $1/T_1T = \text{constant}$, is observed just above T_c . At temperatures below T_c an upturn in $1/T_1T$ is seen only in this doping regime.²¹ A remarkable enhancement of T_c ($\Delta T_c = 20$ K) due to pressure application is attributable to an increase in $D(\epsilon_F)$. In the overdoped regime, other hole pockets, α_1 and α_2 surfaces around the $\Gamma(0,0)$ point, are also expected to become smaller than those in the underdoped regime.²² Therefore, the remarkable T_c enhancement is attributable to an increase in $D(\epsilon_F)$ of the electron pocket, β surface around the M point.

A plateau in $1/T_1T$ just above T_c originates from the electron pocket around the M point and is clearly observed in the overdoped regime compared to the optimally doped regime. This can be explained as follows: the gap between the Fermi energy and the states around the $\Gamma'(\pi, \pi)$ point is larger for $x=0.14$ than for $x=0.10$, as seen from Figs. 1(g) and 1(h). Therefore, a deviation from the plateau in $1/T_1T$ occurs at much higher temperatures (~ 40 K) for $x=0.14$. Thus, the $1/T_1T$ components coming from T -dependent and T -independent $D(\epsilon_F)$ have different origins. This could explain why $1/T_1T$ exhibits a qualitatively different pressure response between low and high temperatures, as shown in Fig. 1(d): $1/T_1T$ at high temperature is suppressed by applying pressure, whereas the plateau in $1/T_1T$ is enhanced by applying pressure.

(5) *Undoped regime* ($x=0.0$). A spin-density-wave-type AF phase is realized for $x < 0.05$.^{2,3,23} In the undoped samples, the structural and AF phase transitions occur at $T_s = 160$ K and $T_N = 140$ K, respectively, at ambient pressure.^{1,2} Pressure-induced superconductivity appears when high pressure is applied: T_c of 21 K is realized at 12 GPa.^{12,24} Although zero resistivity was confirmed at high pressure, a precursor to superconductivity is seen at 2 GPa as a remarkable decrease in resistivity.^{11,12} As Fig. 2 shows, application of pressure reduces AF fluctuation remarkably below T_s . The pressure dependence of the AF fluctuation is completely different from that observed for $x \geq 0.05$. The difference arises from the tetragonal-to-orthorhombic phase transition, which would worsen the nesting condition of the two-dimensional Fermi surface. However, the situation is favorable for the appearance of superconductivity, which develops when the AF fluctuation weakens. In this sense, the pressure-induced superconductivity has the same origin as that realized by F substitution.

The results shown in Figs. 1(a)–1(d) are summarized in the phase diagrams in Figs. 3(a) and 3(b). The values of T_c determined from the onset of the resistivity and $1/T_1T$ [arrows in Figs. 1(a)–1(d)] are plotted in Figs. 3(a) and 3(b). Pressure application enhances low-frequency AF fluctuation in the underdoped or optimally doped regime. The AF fluctuation

accompanied by an increase in T_c has also been observed in FeSe.²⁵ However, the increase in T_c is small in the La1111 series. As the phase diagram at 3.0 GPa shows, superconductivity with $T_c \geq 40$ K develops in the overdoped regime away from the strong AF fluctuation caused by pressure application. This fact calls into question the strong interplay between AF fluctuation and superconductivity. Thus, the question of whether the features observed in the overdoped regime are common to the other 1111 series arises.

The T - x phase diagram at 3.0 GPa is reminiscent of diagrams of the Ce, Pr and Sm 1111 series at ambient pressure in that T_c hardly drops to below 40 K even in the heavily doped regime and the highest T_c is realized away from the AF phase. Figure 4(a) shows a phase diagram normalized by the doping levels, x_{AF} , at which the AF phase vanishes. The values of x_{AF} are estimated as 0.04, 0.06, 0.075, and 0.04 for the La, Ce, Pr, and Sm 1111 series, respectively.^{1–7} The phase diagram includes some ambiguity in the determination of x_{AF} . However, Fig. 4(a) allows comparison of the SC phase boundary because differences due to x -estimation methods are excluded to some extent. As the figure shows, the x/x_{AF} dependence of T_c normalized by the optimal T_c is almost the same for the 1111 series with high T_c above 40 K. Only the La1111 series at ambient pressure deviates from the curve.

The similarity between the La1111 series at 3.0 GPa and the other 1111 series is well understood if the pnictogen height from the basal plane of iron determines T_c , as suggested by a theoretical investigation.¹⁴ According to x-ray diffraction measurements under pressure by Garbarino *et al.*, pnictogen height increases with increasing pressure, and the lattice constant shrinks as well.²⁶ The same changes occur in full rare-earth substitution: the pnictogen height increases in the order of La, Ce, Nd, and Sm, and the lattice constants also shrink in the same order, as shown in Fig. 4(b).^{3,6,27–29} Data for the optimally doped samples are shown as functions of T_c values in the figure. The La1111 series at 3.0 GPa ($T_c = 40$ K) corresponds to the Ce1111 series at ambient pressure. The pnictogen height and lattice parameter estimated from Fig. 4(b) are 0.1565 and 3.97 Å, respectively. According to the x-ray diffraction measurements on the La1111 series, the former and latter are estimated to be 0.158 and 3.97 Å, respectively, at 3.16 GPa.²⁶ The agreement is fairly good, therefore, pressure application and full rare-earth substitution are equivalent, and the phase diagram determined under pressure is common to the 1111 series with high T_c above 40 K.

In some respects, pressure application to the La1111 series is more useful than full rare-earth substitution because pressure is a cleaner and more continuous parameter on the phase diagram. It also allows investigation of the high- T_c mechanism in the other 1111 series. When the 1111 series with high T_c (≥ 40 K) at ambient pressure are viewed in terms of the present measurements under pressure, high T_c is realized away from the AF fluctuation which should be stronger than that of the La1111 series at the same doping level. Unfortunately, this expectation is not clearly confirmed by NMR measurements because magnetic fluctuation arising from rare-earth ions predominates, which prevents the extraction of AF fluctuation arising from the basal planes of iron.

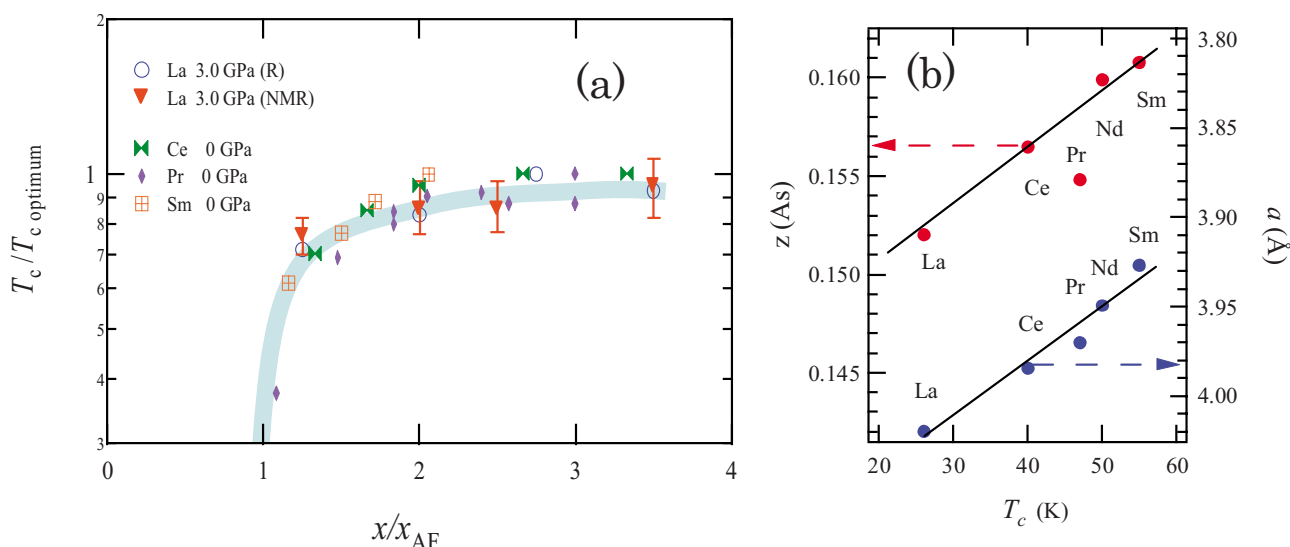


FIG. 4. (Color online) (a) T_c for various $\text{RFeAsO}_{1-x}\text{F}_x$. T_c and x are normalized by the optimal T_c and the antiferromagnetic phase boundary x_{AF} , respectively. Blue open circles and red closed triangles represent T_c determined from the resistivity and $1/T_1T$ at 3.0 GPa, respectively [see Fig. 3(b)]. (b) Pnictogen height measured from the basal plane of iron and lattice constant of the plane for the $R1111$ series ($R=\text{La, Ce, Pr, Nd, and Sm}$). Data for the optimally doped samples are plotted as functions of T_c values. T_c of the La1111 series at 3.0 GPa is 40 K. The corresponding pnictogen height and lattice constant are 0.1565 and 3.97 Å, respectively, as indicated by arrows.

In summary, the critical doping level of the La1111 series is estimated as $x \sim 0.10$ from $1/T_1T$ at ambient pressure and 3.0 GPa. The phase diagram at 3.0 GPa indicates that superconductivity with $T_c \geq 40$ K develops in the overdoped regime away from the strong AF fluctuation. Pressure applica-

tion is equivalent to full rare-earth substitution, suggesting that high T_c above 40 K in the 1111 series originates not from the AF fluctuation but from $D(\varepsilon_F)$ at the electron pocket around the M point.

*naoki@fujiwara.h.kyoto-u.ac.jp

[†]Present address: Department of Applied Physics & Physico-Informatics, Faculty of Science & Technology, Keio University.

[‡]Present address: Department of Mechanical Engineering and Intelligent Systems Faculty of Engineering, Tohoku Gakuin University.

¹Y. Kamihara *et al.*, *J. Am. Chem. Soc.* **130**, 3296 (2008).

²H. Luetkens *et al.*, *Nature Mater.* **8**, 305 (2009).

³Q. Huang, J. Zhao, J. W. Lynn, G. F. Chen, J. L. Luo, N. L. Wang, and P. Dai, *Phys. Rev. B* **78**, 054529 (2008).

⁴Y. Kamihara *et al.*, *New J. Phys.* **12**, 033005 (2010).

⁵C. Hess *et al.*, *EPL* **87**, 17005 (2009).

⁶J. Zhao *et al.*, *Nature Mater.* **7**, 953 (2008).

⁷C. R. Rotundu, D. T. Keane, B. Freelon, S. D. Wilson, A. Kim, P. N. Valdivia, E. Bourret-Courchesne, and R. J. Birgeneau, *Phys. Rev. B* **80**, 144517 (2009).

⁸H. Chen *et al.*, *EPL* **85**, 17006 (2009).

⁹B. Lv, M. Gooch *et al.*, *New J. Phys.* **11**, 025013 (2009).

¹⁰F. Rullier-Albenque, D. Colson, A. Forget, and H. Alloul, *Phys. Rev. Lett.* **103**, 057001 (2009).

¹¹H. Takahashi *et al.*, *Nature (London)* **453**, 376 (2008).

¹²H. Okada *et al.*, *J. Phys. Soc. Jpn.* **77**, 113712 (2008).

¹³C. H. Lee *et al.*, *J. Phys. Soc. Jpn.* **77**, 083704 (2008).

¹⁴K. Kuroki, H. Usui, S. Onari, R. Arita, and H. Aoki, *Phys. Rev. B* **79**, 224511 (2009).

¹⁵S. Onari and H. Kontani, *Phys. Rev. Lett.* **103**, 177001 (2009).

¹⁶H. Kontani and S. Onari, *Phys. Rev. Lett.* **104**, 157001 (2010).

¹⁷K. Kuroki, S. Onari, R. Arita, H. Usui, Y. Tanaka, H. Kontani,

and H. Aoki, *Phys. Rev. Lett.* **101**, 087004 (2008).

¹⁸I. I. Mazin, D. J. Singh, M. D. Johannes, and M. H. Du, *Phys. Rev. Lett.* **101**, 057003 (2008).

¹⁹H. Ikeda, *J. Phys. Soc. Jpn.* **77**, 123707 (2008).

²⁰H.-J. Grafe, D. Paar, G. Lang, N. J. Curro, G. Behr, J. Werner, J. Hamann-Borrero, C. Hess, N. Leps, R. Klingeler, and B. Buchner, *Phys. Rev. Lett.* **101**, 047003 (2008).

²¹T. Nakano, N. Fujiwara, K. Tatsumi, H. Okada, H. Takahashi, Y. Kamihara, M. Hirano, and H. Hosono, *Phys. Rev. B* **81**, 100510(R) (2010).

²²H. Ikeda, R. Arita, and J. Kunes, *Phys. Rev. B* **81**, 054502 (2010).

²³C. de la Cruz *et al.*, *Nature (London)* **453**, 899 (2008).

²⁴T. Kawakami *et al.*, *J. Phys. Soc. Jpn.* **78**, 123703 (2009).

²⁵T. Imai, K. Ahilan, F. L. Ning, T. M. McQueen, and R. J. Cava, *Phys. Rev. Lett.* **102**, 177005 (2009).

²⁶G. Garbarino, P. Toulemonde, M. Alvarez-Murga, A. Sow, M. Mezouar, and M. Nunez-Regueiro, *Phys. Rev. B* **78**, 100507(R) (2008).

²⁷J. Zhao, Q. Huang, C. de la Cruz, J. W. Lynn, M. D. Lumsden, Z. A. Ren, J. Yang, X. Shen, X. Dong, Z. Zhao, and P. Dai, *Phys. Rev. B* **78**, 132504 (2008).

²⁸Y. Qiu, W. Bao, Q. Huang, T. Yildirim, J. M. Simmons, M. A. Green, J. W. Lynn, Y. C. Gasparovic, J. Li, T. Wu, G. Wu, and X. H. Chen, *Phys. Rev. Lett.* **101**, 257002 (2008).

²⁹S. Margadonna, Y. Takabayashi, M. T. McDonald, M. Brunelli, G. Wu, R. H. Liu, X. H. Chen, and K. Prassides, *Phys. Rev. B* **79**, 014503 (2009).